

## Book Chapter

# Nanocrystalline FeMnO<sub>3</sub> Powder as Catalyst for Combustion of Volatile Organic Compounds

Corneliu Doroftei

Science Research Department, Institute of Interdisciplinary Research, Research Center in Environmental Sciences for the North-Eastern Romanian Region (CERNESIM), Alexandru Ioan Cuza University of Iasi, Bulevardul Carol I, Nr. 11, 700506 Iasi, Romania

**\*Corresponding Author:** Corneliu Doroftei, Science Research Department, Institute of Interdisciplinary Research, Research Center in Environmental Sciences for the North-Eastern Romanian Region (CERNESIM), Alexandru Ioan Cuza University of Iasi, Bulevardul Carol I, Nr. 11, 700506 Iasi, Romania

Published **October 30, 2024**

This Book Chapter is a republication of an article published by Corneliu Doroftei, et al. at Nanomaterials in March 2024. (Doroftei, C. Nanocrystalline FeMnO<sub>3</sub> Powder as Catalyst for Combustion of Volatile Organic Compounds. Nanomaterials 2024, 14, 521. <https://doi.org/10.3390/nano14060521>)

**How to cite this book chapter:** Corneliu Doroftei. Nanocrystalline FeMnO<sub>3</sub> Powder as Catalyst for Combustion of Volatile Organic Compounds. In: Tenderwealth Clement Jackson, editor. Prime Archives in Nanotechnology. Hyderabad, India: Vide Leaf. 2024.

© The Author(s) 2024. This article is distributed under the terms of the Creative Commons Attribution 4.0 International License (<http://creativecommons.org/licenses/by/4.0/>), which permits

unrestricted use, distribution, and reproduction in any medium, provided the original work is properly cited.

**Funding:** This research received no external funding.

**Conflicts of Interest:** The author declares no conflict of interest.

## Abstract

The paper shows the obtaining of nanocrystalline iron manganite ( $\text{FeMnO}_3$ ) powders and its investigation in terms of catalytic properties for a series of volatile organic compounds. The catalyst properties were tested in the catalytic combustion of air-diluted vapors of ethanol, methanol, toluene and xylene at moderate temperatures (50 – 550 °C). Catalytic combustion of the alcohols starts at slightly higher temperature (180 – 230 °C), the conversion of ethanol vapors starts at 230 °C and increases rapidly around 97% with the temperature increase in the range of 230 – 300 °C. For temperatures higher than 300 °C, the degree of conversion is kept at the same value. In the case of methanol vapors, the conversion starts at a slightly lower temperature (180 °C) and the degree of conversion reaches the value of 97% at a higher temperature (440 °C) than in the case of ethanol, and it also remains constant as the temperature increases. Catalytic combustion of the hydrocarbons starts at lower temperatures (around 50 °C), the degree of conversion is generally lower and it increases proportionally with the temperature, with the exception of toluene, which shows an intermediate behavior, reaching values of over 97% at 430 °C. The studied iron manganite can be recommended to achieve catalysts that operate at moderate temperatures for the combustion of some alcohols and, especially, ethanol. The performance of this catalyst with regard to ethanol is close to that of a catalyst that uses noble metals in its composition.

## Keywords

Nanocrystalline  $\text{FeMnO}_3$ ; sol-gel self-combustion; structural properties; catalytic combustion; volatile organic compounds

## 1. Introduction

In general, catalysts are used when the concentration of combustible gases in the air is very low and cannot support combustion with a flame. Catalytic combustion at low and medium temperature is used to remove polluting gases from the air, volatile organic compounds (VOCs) such as solvent vapors, mine gases, combustible gases escaped from industrial installations etc. Established and widely used materials as combustion catalysts are a number of noble metals: platinum, iridium, palladium, rhodium, gold, their alloys with other metals, deposits of such metals on metal or ceramic supports, etc. Recent research on these catalysts aims to improve the methods of their preparation and use [1–5]. The aim is to achieve a large specific area, increase the thermal and chemical stability and the duration of use, for example by embedding in a ceramic matrix some nanometric particles of metal catalyst [1,2]. The temperature stability of metal catalysts is limited by their volatility [6]. Due to the high cost of noble metals their use as combustion catalysts is limited especially to industrial processes, where noble metals from spent catalysts are recovered.

In recent years, remarkable catalytic properties have been discovered in a number of oxide compounds: oxides of some metals, ferrites, perovskites etc.

One of the first oxide catalysts studied was the simple  $\text{CuCoO}_3$  perovskite on a  $\gamma\text{Al}_2\text{O}_3$  support. Compared with a classic platinum catalyst, the elimination of propylene from the exhaust air from the polypropylene processing installations was analyzed. It was found that the new catalyst can successfully replace the platinum catalyst [7].

Another nanostructured perovskite,  $\text{PrCrO}_3$  on a  $\text{CeO}_2$  support, prepared by the urea combustion method, was tested in the post-combustion of diesel engine exhaust gases. The results are similar to those of a platinum catalyst on alumina support [8].

An invention patent proposes the use as combustion catalysts of complex perovskites with rare earths, the recommended

compositions being those of the  $\text{La}_x\text{A}_y\text{B}_z\text{O}_{3-\delta}$  type (with oxygen deficiency). The A ion can be strontium, calcium or copper, and the B ion can be cobalt, manganese, chromium or iron. The support according to the invention is a complex mineral called mullite ( $3\text{Al}_2\text{O}_3 \cdot 2\text{SiO}_2 - 2\text{Al}_2\text{O}_3 \cdot 3\text{SiO}_2$ ) prepared in the form of microspheres with a diameter of 20 – 200 nm and sintered at 1300 – 1500 °C. The preparation method involves the impregnation of mullite, pressed in the desired form for the catalyst, with solutions of nitrates or acetates of the cations and calcination at 500 – 700 °C. Thus, effective catalysts were obtained for the depollution of exhaust gases from internal combustion engines, both with gasoline and diesel, at working temperatures below 300 °C [9].

High performances were obtained by a substitution with silver in the perovskite with the composition  $\text{La}_{0.88}\text{Ag}_{0.12}\text{FeO}_3$  obtained by grinding in a high-energy mill, on an  $\text{Al}_2\text{O}_3$  alumina support. It was found both the reduction of nitrogen oxides and the complete oxidation of hydrocarbons at temperatures of 400 – 500 °C [10].

Huang et al prepared  $\text{La}_{0.8}\text{Cu}_{0.2}\text{MnO}_3$  and  $\text{La}_{0.8}\text{Sr}_{0.2}\text{MnO}_3$  for toluene elimination in the presence of dodecyl-mercaptan and both catalysts lost activity over time due to the formation of  $\text{CuSO}_4$  or  $\text{SrSO}_4$  [11,12].

Also, a patent proposes the use of manganese-copper spinel ferrite in the form of nanometric particles as a low temperature combustion catalyst in cigarette filters [13].

A complex oxide compound is described in a patent that proposes a highly active combustion catalyst. A nanostructured cerium-aluminum complex oxide is deposited on an aluminum oxide support, over which a copper-aluminum complex oxide is deposited. The catalyst is able to reduce the nitrogen oxides from the burnt gases [14].

The performance of catalytic combustion it is very much influenced by the type of catalyst used. The preparation of catalysts with nanosized particles is the key to an efficient catalytic performance. In nanostructured materials, the interface

between nanoparticles and surrounding medium plays a more important role than in the bulk materials [15].

In this work the porous nanocrystalline iron manganite was synthesized by sol-gel self-combustion technique using metal nitrates corresponding to the studied compound and polyvinyl alcohol was used as colloidal medium [16–18]. The catalyst properties were tested in the catalytic combustion of air-diluted vapors of ethanol ( $C_2H_5OH$ ), methanol ( $CH_3OH$ ), toluene ( $C_6H_5CH_3$ ) and xylene ( $C_8H_{10}$ ) at moderate temperatures (50 – 550 °C).

## 2. Materials and Methods

Nanocrystalline iron manganite ( $FeMnO_3$ ) was obtained by sol-gel self-combustion method [18] using iron(III) nitrate nonahydrate, manganese(II) nitrate tetrahydrate, ammonium hydroxide solution and poly(vinyl alcohol) (PVA) solution. The solutions of iron and manganese nitrates in stoichiometric quantities were mixed with a solution of poly(vinyl alcohol) forming a colloidal mixture. Ammonium hydroxide solution was added until a soil of metal hydroxides with  $pH = 8$  were formed. The resulting soil was dried at a temperature of 150 °C, and then ignited locally, an exothermic combustion reaction taking place. Following the combustion with spontaneous self-propagation, iron manganite resulted in the form of nanocrystalline powder. The powder was subsequently calcined at 500 °C for 30 min and then it was subjected to a heat treatment in air at 1000 °C for 7 h.

The iron manganite powder obtained after the heat treatment was investigated by thermogravimetric (TG) and differential thermal analysis (DTA) in the temperature range 25 – 1000 °C at a heating rate of 10 °C/min in static air, by X-ray diffraction measurements (XRD), by scanning electron microscopy with energy dispersive X-ray spectroscopy (SEM/EDX), by X-ray photoelectron spectroscopy (XPS) and by measurements using the Brunauer, Emmet and Teller method (BET).

The measurements regarding the catalytic activity for the selected VOCs (ethanol, methanol, toluene and xylene) were carried out at

moderate temperatures (50 – 550 °C) in a flow-type set-up, previously described in ref. [19]. The catalyst in the form of powder (0.5 g) was introduced into a tubular quartz reactor ( $\varnothing = 8$  mm) with automatic temperature control, so that the input gas flow (gas flow rate of 100 cm<sup>3</sup>/min, VOC concentration in air of 1-2‰ and the gas hourly space velocity, GHSV, of 5200 h<sup>-1</sup>) to pass through the entire volume of the powder, at a pressure close to atmospheric pressure. The degree of conversion  $C$  of the gas leaving the reactor was determined as [20]:

$$C = (c_{in} - c_{out})/c_{in} \times 100 (\%), \quad (1)$$

where  $c_{in}$  is the concentration of the gas at the reactor inlet and  $c_{out}$  is the gas concentration at the reactor outlet, measured by a detection system with photoionization (PID-TECH) for gases and VOCs. In order to obtain information on the degree of stability of the catalyst, the experiments were carried out both at an increase in temperature and at a decrease in temperature. These determinations were repeated and similar results were obtained, indicating the stability of the catalyst material over time, without its deactivation.

### 3. Results and Discussions

#### 3.1. Structure and Morphology

The powder resulting from the self-combustion reaction has been investigated by TG-DTA analyses. From the obtained data (Figure 1) it is evident that the mass of the powder decreases slightly (0.13%) with the increase in temperature up to around 300 °C as a result of the loss of volatile substances.

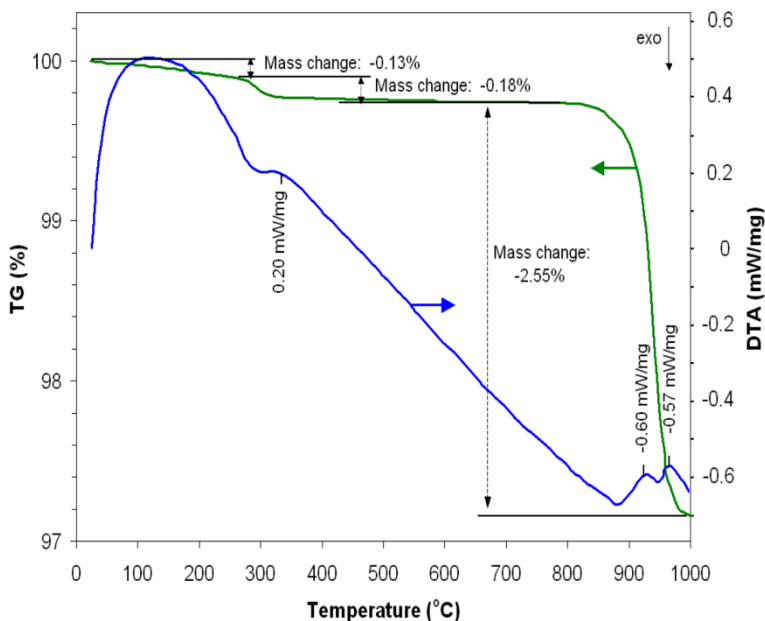


**Figure 1.** TG-DTA of synthesizing iron manganite.

Corresponding to the temperature of 330 °C, the DTA curve indicates the presence of an endothermic peak that can be interpreted by the production of some crystallization reactions that correspond to a decrease in the powder mass by 0.18%. The crystalline phases of iron manganite begin to appear at temperatures above 900 °C. Thus, one can notice an endothermic peak at 930 °C corresponding to a considerable decrease in the mass of the powder (2.55%) followed by another endothermic peak at 970 °C where the mass tend to remain constant indicating the formation of the crystalline structure of iron manganite. Taking into account this information and aiming to obtain a material with good crystallinity, the powder was heat treated at 1000 °C for 7 h.

The X-ray diffraction measurements made for the heat-treated powder at these parameters confirm the obtaining of iron manganite with a perovskite type structure with good crystallinity without secondary phases (Figure 2a). The X-ray diffractogram (CuK $\alpha$  radiation source, wavelength  $\lambda = 1.54182 \text{ \AA}$ ) was indexed

according to the PDF card No. 75–894 for the iron manganite perovskite. The (211), (222), (123), (400), (411), (332), (422), (431), (125), (440), (611), (026), (145), (622), (134) and (444) peaks reveal that the powder has a cubic perovskite phase with  $la3$  space group, without any foreign phase. The value obtained for the lattice parameter ( $a = b = c = 9.40 \text{ \AA}$ ) is close to the values obtained by other authors ( $a = 9.40 \text{ \AA}$ ) [21], ( $a = 9.41 \text{ \AA}$ ) [22,23], who synthesized the iron manganite by different methods. The representation of the spatial structure of the unit cell is given in Figure 2b [24–26].

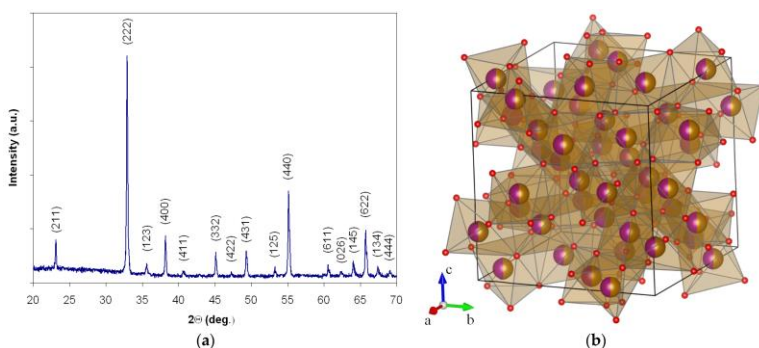


**Figure 2:** The X-ray diffractogram (a) and 3D representation of the unit cell in  $la3$  symmetry for iron manganite (b). Iron ions are orange, manganese ions are purple halves of the balls, and oxygen ions are red balls.

Iron is at the site 8b, manganese is at site 24d and oxygen is placed at site 48e. Manganese and iron occupy 50% of the sites 8b and 24d respectively, that is, at both 8b and 24d site, there is equal occupation of manganese and iron (i.e.,50:50) [22,25].

The iron manganite powder obtained by the sol-gel self-combustion route using PVA as a colloidal medium and subsequently heat treated at  $1000 \text{ }^\circ\text{C}$  for 7 h shows a structure with fine granulation (100 – 500 nm) and accentuated porosity in which open pores predominate (Figures 3a-c). Also, from the SEM micrographs, a clustered structure of the granules in mini- or macro-agglomerations with irregular shapes and sizes can be highlighted. According to the BET analyses, the specific surface area ( $S_{\text{BET}}$ ) and the average crystallite size ( $D_{\text{BET}}$ ) have a value of  $3.20 \text{ m}^2/\text{g}$  and 370 nm, respectively (Figure 3d).



Heterogeneous catalysis being a surface phenomenon, its efficiency is determined both by the chemical composition and the structure of the catalyst surface. A nanometric structure ensures a large specific surface area and a superior reactivity of the catalyst [27].

The elemental composition and homogeneity of the studied material was confirmed by the energy dispersive X-ray (EDX) spectra (Figure 3e). In the composition of the material, only the elements Fe, Mn and O are found and as can be deduced, the value of the  $\text{Fe(at\%)/[Fe(at\%)+Mn(at\%)]}$  or  $\text{Mn(at\%)/[Fe(at\%)+Mn(at\%)]}$  ratio is close to 0.5.

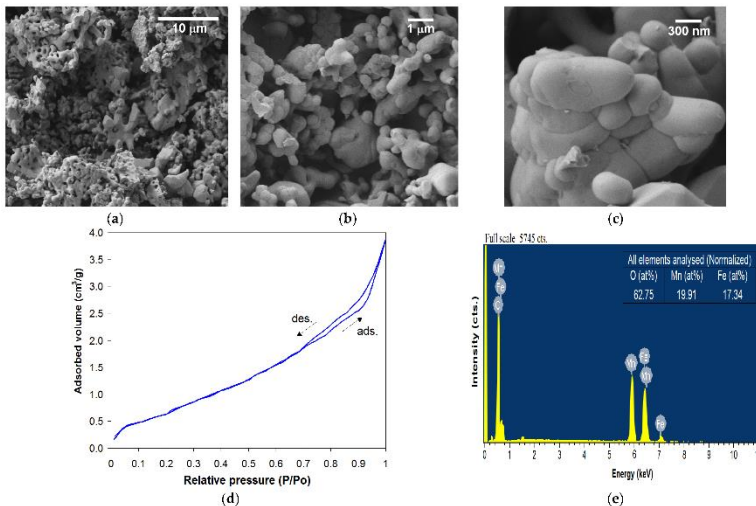


**Figure 3:** SEM micrographs obtained at different magnifications (a-c), BET adsorption –desorption isotherm (d) and EDX spectrum with the analysed elements (e) for iron manganite heat treated at 1000 °C / 7h.

X-ray photoelectron spectroscopy (XPS) using Al-K $\alpha$  radiation, is used to investigate the oxidation state of the cations as well as the existence of oxygen vacancies on the surface of the material that play an important role in terms of its catalytic activity [28]. Presented in Figure 4 are the XPS spectra and their deconvolution, attributed to the presence of iron in 2p<sub>1/2</sub> and 2p<sub>3/2</sub> (a), manganese in 2p<sub>1/2</sub> and 2p<sub>3/2</sub> (b) and oxygen in 1s (c).

The spectrum attributed to iron (Figure 4a) is highlighted by two main peaks located at 724.44 eV ( $2p_{1/2}$ ) and 710.84 eV ( $2p_{3/2}$ ) preceded by satellite peaks located at 732.64 eV and 719.04 eV respectively. From the deconvolution of the spectrum, it appears that the iron is found in the  $Fe^{3+}$  oxidation state, confirmed by the presence of the two satellite peaks that follow the main peaks and the deconvolution peaks located at 727.44 eV and at 713.84 eV. Also, iron is also found in the  $Fe^{2+}$  oxidation state, confirmed by the deconvolution peaks located at 724.24 eV and 710.64 eV [29,30].

The spectrum attributed to manganese (Figure 4b) is also highlighted by two main peaks located at 652.84 eV ( $2p_{1/2}$ ) and 641.44 eV ( $2p_{3/2}$ ) and from the deconvolution analysis of the spectrum it appears that manganese is found in the  $Mn^{3+}$  oxidation state [31,32].

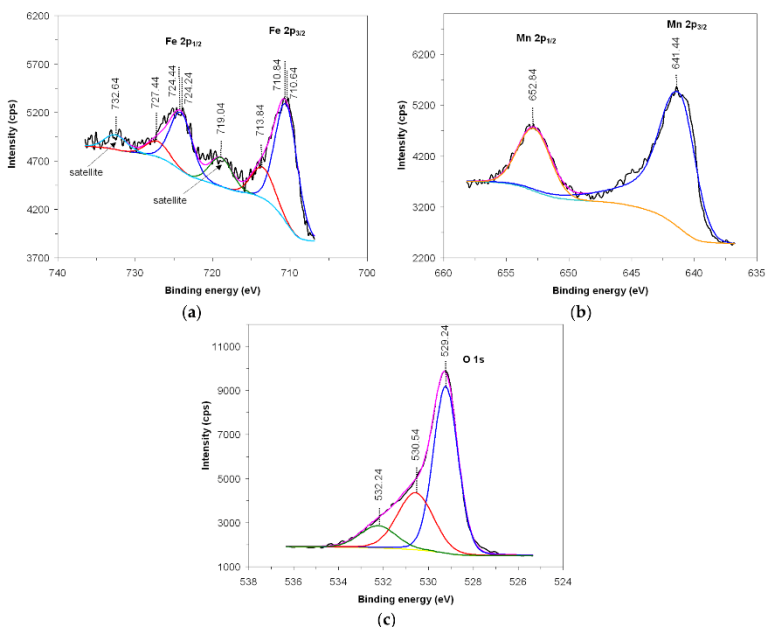


**Figure 4:** XPS spectrum of Fe 2p (a), Mn 2p (b) and O 1s (c).

Also, the spectrum attributed to oxygen (Figure 4c) is highlighted by an asymmetric main peak located at 529.24 eV (1s), this is specific for transition metal oxides and is also favored by the presence of iron in the  $\text{Fe}^{2+}$  oxidation state, indicating the presence of oxygen vacancies [33]. The deconvolution analysis of the spectrum reveals the presence of three oxygen species,  $\text{OH}^{\cdot}/\text{O}^2$ ,  $\text{O}_2^{\cdot-}/\text{O}^-$  or  $\text{O}^{2-}$ , attributed to the peaks located at 532.24 eV, 530.54 eV and 529.24 eV, respectively.

## 3.2. Catalytic Activity

The results of the measurements regarding the catalytic combustion at moderate temperatures of alcohols (ethanol and methanol) and hydrocarbons (toluene and xylene) diluted in air using iron manganite as a catalyst in the form of powder are presented in Figures 5, 6 and Table 1. Figure 5 shows the degree of conversion as a function of the reaction temperature for catalytic flameless combustion of the studied VOCs.

Typical S-shaped curves were obtained, which describe the variation of the degree of conversion with increasing reaction temperature. These curves indicate that the catalytic activity of iron manganite is much more strongly influenced by the reaction temperature in the case of alcohols than in the case of hydrocarbons. Moreover, the catalytic activity of alcohols begins at higher temperatures than that of the studied hydrocarbons.

The conversion of ethanol vapors starts at 230 °C and increases rapidly around 97% with the temperature increase in the range of 230 – 300 °C. For temperatures higher than 300 °C, the degree of conversion is kept at the same value. In the case of methanol vapors, the conversion starts at a slightly lower temperature (180 °C) and the degree of conversion reaches the value of 97% at a higher temperature (440 °C) than in the case of ethanol, and it also remains constant as the temperature increases.

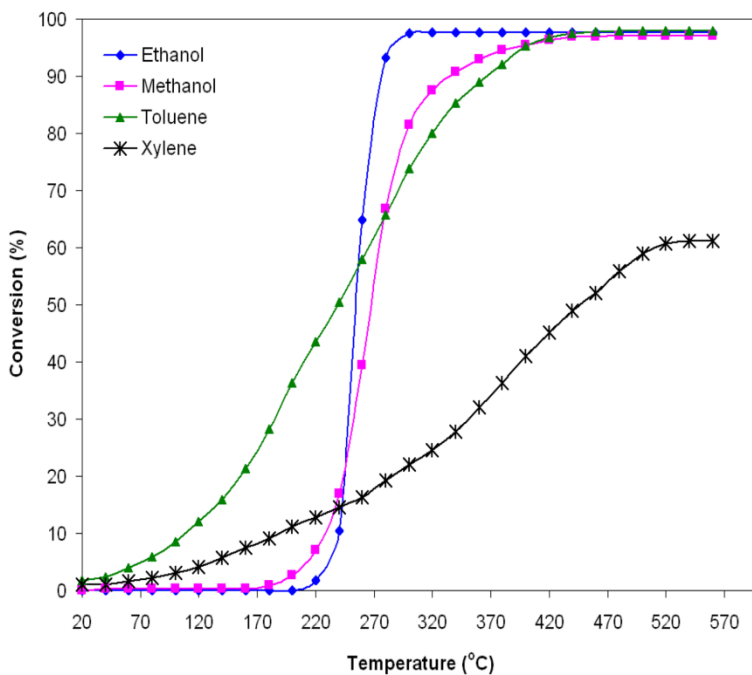


**Figure 5:** Conversion of ethanol, methanol, toluene and xylene as a function of the operating temperature of the  $\text{FeMnO}_3$  catalyst (1-2% VOC in air, 0.5 g catalyst and  $\text{GHSV} = 5200 \text{ h}^{-1}$ ).

For the studied hydrocarbons (toluene and xylene), the conversion starts at temperatures lower than 50 °C. The degree of conversion increases up to the value of 97.5% at 430 °C for toluene and only 60% at 520 °C for xylene, after which it remains constant.

To estimate the catalytic activity of a catalyst, the temperature required for 10% gas conversion ( $T_{10}$ ) when the catalytic reaction is started and is stable is taken into account, as well as the temperature required for 50% gas conversion ( $T_{50}$ ), which is usually chosen as the main indicator of the catalytic activity of a given catalyst [19]. The values of these temperatures are presented in Figure 6 for all tested volatile organic compounds. The lowest  $T_{10}$  temperatures were obtained in the case of hydrocarbons, 110 °C and 190 °C for toluene and xylene respectively, followed by alcohols where the values of these temperatures are very close, 230 °C and 240 °C for methanol and ethanol respectively.

At  $T_{50}$ , the catalytic activity is high enough and the interactions between the catalyst surface and the reactants are intense. It can be stated that the iron manganite catalyst obtained by the method mentioned above has a high catalytic activity for ethanol, methanol and toluene, while for xylenes it is much lower. The performance of this catalyst is remarkable with regard to ethanol (Figure 5), it approaches that of a catalyst that uses noble metals in its composition. Deng Qian et al. [34] carried out a study on the catalytic combustion of ethanol using catalysts based on  $\text{Au}/\gamma\text{-Fe}_2\text{O}_3$ . With such a catalyst, a conversion value of 99.6% can be achieved for ethanol at a temperature of 290 °C. Also a study carried out by Avgouropoulos et al. [35] regarding the catalytic combustion of ethanol using catalysts based on  $\text{Pt}/\text{Al}_2\text{O}_3$  highlights a conversion value of 90% at a temperature of 220 °C.

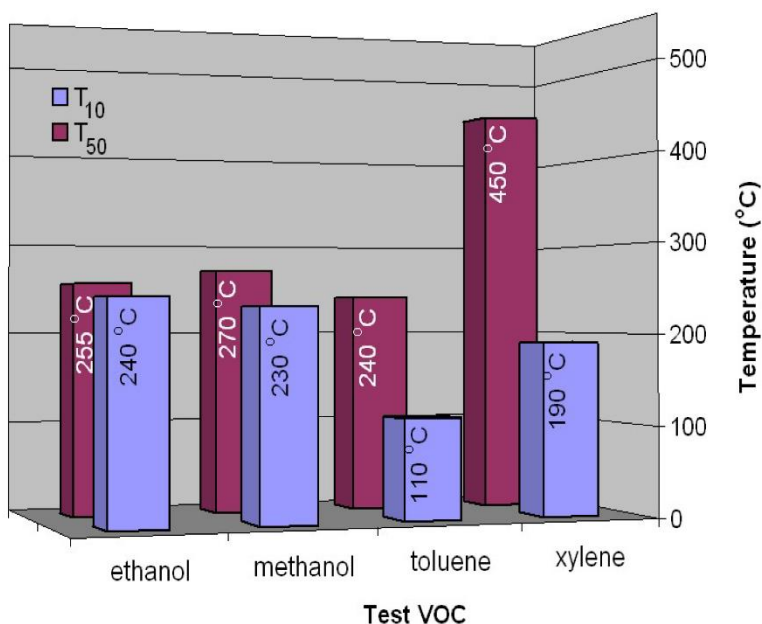


**Figure 6:**  $T_{10}$  and  $T_{50}$  temperatures versus tested VOCs for the  $\text{FeMnO}_3$  catalyst.

The catalytic activity of the  $\text{FeMnO}_3$  catalyst in the conversion of ethanol, methanol, toluene and xylene can be largely attributed to the mobility of oxygen inside the perovskite lattice due to the

oxygen vacancies generated by the presence of iron ions with variable valence,  $\text{Fe}^{2+}/\text{Fe}^{3+}$ , as it could be ascertained from the analysis of the XPS spectrum (Figure 4). Oxygen vacancies favor the appearance of oxygen ion species adsorbed on the iron manganite surface. Although the mechanism regarding the catalytic activity of oxide compounds with a perovskite structure is still under debate, according to some widely accepted opinions, at low temperatures ( $< 400\text{ }^\circ\text{C}$ ), the catalytic activity of oxide compounds with a perovskite structure in total oxidation reactions of gases is to a large extent determined by the amount of weakly bound surface oxygen species [15,36], which in the present case are assumed to be much more available for the oxidation of alcohols (ethanol and methanol) compared to those for the oxidation of hydrocarbons (toluene and xylene). The weaker the oxygen bond on the catalyst surface, the more active the catalyst is for the complete oxidation of gases [15,36,37]. Of course, the roles of specific surface area and particle size are very important. A large specific surface area that can be obtained by an appropriate preparation method of nanomaterials, in the present case the sol-gel self-combustion method, will involve much more interactions between the iron manganite surface and the tested VOCs and, therefore, a high catalytic activity towards their combustion.

The apparent activation energies  $E_a$  of the catalyst in the combustion reactions of ethanol, methanol, toluene and xylene were determined using Arrhenius curves (the natural logarithm of the reaction rate constant  $k$  at low conversion, below 15%, as a function of the inverse of the absolute temperature,  $1/T$ ) [15]. This graph is a straight line, and from its slope the apparent activation energy was calculated [15,37].

Table 1 shows the values of the degree of conversion at two temperatures,  $290\text{ }^\circ\text{C}$  and  $500\text{ }^\circ\text{C}$ , as well as the values of the kinetic parameters (apparent activation energy and reaction rate) for the oxidation of VOCs studied by the  $\text{FeMnO}_3$  catalyst. The values of the apparent activation energies are higher in the case of alcohols and lower in the case of hydrocarbons (Table 1) [38–45], also the catalytic activity starts at much higher temperatures in the case of alcohols compared to that of hydrocarbons (Figure 5).

The reaction rate normalized to the specific surface area can characterize the specific catalytic activity. A catalyst is more active the higher the reaction rate. The reaction rate changes substantially from  $1.07 \times 10^{-2} \mu\text{mol s}^{-1}\text{m}^{-2}$  to  $14.25 \times 10^{-2} \mu\text{mol s}^{-1}\text{m}^{-2}$  depending on the gas type. The highest value of the reaction rate ( $14.25 \times 10^{-2} \mu\text{mol s}^{-1}\text{m}^{-2}$ ) was obtained for the combustion of ethanol by the studied catalyst, it demonstrated the best catalytic activity in the combustion of ethanol (95.43% degree of conversion at 290 °C reaching 97.5% for temperatures higher than 300 °C). The lowest value of the reaction rate ( $1.07 \times 10^{-2} \text{mmol s}^{-1}\text{m}^{-2}$ ) was obtained for the combustion of xylene, the catalyst also showing the weakest catalytic activity in xylene conversion (59% degree of conversion at 500 °C) as can be seen in Figure 5.

**Table 1:** Parameters of the degree of conversion and kinetic parameters

VOCs/ FeMnO <sub>3</sub>	Conversion at 290 °C (%)	Conversion at 500 °C (%)	Reaction rate* ( $\mu\text{mol s}^{-1}\text{m}^{-2}$ )	Activation energy** (KJ/mol)
Ethanol	95.43	97.58	$14.25 \times 10^{-2}$	195.248
Methanol	74.09	97.05	$6.27 \times 10^{-2}$	99.816
Toluene	70.25	97.91	$5.55 \times 10^{-2}$	19.477
Xylene	20.63	59.00	$1.07 \times 10^{-2}$	18.232

\*Reaction rate (at 290 °C) for VOC concentration at low conversion per unit surface area of catalyst

\*\*Apparent activation energy for low conversions

The values obtained for the kinetic parameters in the case of the studied oxidic compound as a catalyst for ethanol, methanol, toluene and xylene vapors are comparable to the values reported in the literature for a series of oxidic compounds with a similar structure and VOCs [39–41,46].

From the obtained results, it can be stated that the porous oxide compound with a perovskite type structure (FeMnO<sub>3</sub>) obtained by sol-gel self-combustion method can be a promising candidate for the realization of catalysts that operate at moderate temperatures for the combustion of some alcohols, especially ethanol.

## 4. Conclusions

The paper shows the obtaining of iron manganite ( $\text{FeMnO}_3$ ) in the form of a nanometric powder with high purity and crystallinity and its investigation from the point of view of its catalytic properties for a series of volatile organic compounds (ethanol, methanol, toluene and xylene) at moderate temperatures (50 – 550 °C).

The conversion of ethanol vapors starts at 230 °C and increases rapidly around 97% with the temperature increase in the range of 230 – 300 °C. For temperatures higher than 300 °C, the degree of conversion is kept at the same value. In the case of methanol vapors, the conversion starts at a slightly lower temperature (180 °C) and the degree of conversion reaches the value of 97% at a higher temperature (440 °C) than in the case of ethanol, and it also remains constant as the temperature increases.

In the case of the studied hydrocarbons (toluene and xylene), the conversion starts at temperatures lower than 50 °C. The degree of conversion increases up to the value of 97.5% at 430 °C for toluene and only 60% at 520 °C for xylene, after which it remains constant.

The studied iron manganite can be recommended to achieve catalysts that operate at moderate temperatures for the combustion of some alcohols, especially ethanol. The performance of this catalyst in terms of ethanol approaches that of a catalyst that uses noble metals in its composition.

## References

1. Masatake H. When gold is not noble: Catalysis by nanoparticles, *The Chemical Record*. 2003; 3: 75–87.
2. Suzuki Y, Horii Y, Kasagi N. Microcatalytic combustor with tailored  $\text{Pt}/\text{Al}_2\text{O}_3$  films, In: *Proceedings of the 3rd International Workshop on Micro and Nanotechnology for Power Generation and Energy Conversion Applications (Power MEMS 2003)*. 4–5 December 2003; Makhuri; Japan, 23–26.



3. Pecchi G, Reyes P, Figueroa A, Fierro JLG. Catalytic combustion on toluene on Pd-Cu/SiO<sub>2</sub> catalysts. *Bol. Soc. Chil. Quím.* 2000; 45: 213–2018.
4. Andreeva D, Petrova P, Ilieva L, Sobczak JW, Abrashev MV. Design of new gold catalysts supported on mechanochemically activated ceria-alumina, promoted by molybdena for complete benzene oxidation. *Applied Catalysis B: Environmental.* 2008; 77: 364–372.
5. Persson K, Ersson A, Jansson K, Iverlund N, Jaras S. Influence of co-metals on bimetallic palladium catalysts for methane combustion. *Journal of Catalysis.* 2005; 231: 139–150.
6. Svensson EE. Nanomaterials for high-temperature catalytic combustion, Thesis in Chemical Engineering. KTH chemical Science and Engineering, Stockholm, Sweden. 2007.
7. Haber J, Mielczarska E, Turek W. Oxide catalyst for the combustion of organic compounds in industrial waste gases. *Reaction Kinetics and Catalysis Letters.* 1987; 34: 45–49.
8. Fino D, Specchia V. Compositional and structural optimal design of a nanostructured diesel-soot combustion catalyst for a fast-regenerating trap. *Chemical Engineering Science.* 2004; 59: 4825–4831.
9. Tang Y, Lin B. Perovskite-type rare earth complex oxide combustion catalysts, United States Patent No. 5242881. 2005.
10. Zhang R, Alamdari H, Bassir M, Kaliaguine S. Optimization of mixed Ag catalysts for catalytic conversions of NO and C<sub>3</sub>H<sub>6</sub>. *International Journal of Chemical Reactor Engineering.* 2007; 5: Article A70.
11. Huang HF, Sun Z, Lu HF, Shen LQ, Chen YF. Study on the poisoning tolerance and stability of perovskite catalysts for catalytic combustion of volatile organic compounds. *Reaction Kinetics Mechanisms and Catalysis.* 2010; 101: 417–427.
12. Tomatis M, Xu HH, He J, Zhang XD. Recent development of catalysts for removal of volatile organic compounds in flue gas by combustion: A Review. *Journal of Chemistry* 2016; Article ID 8324826, 1–15.

13. Shalva G. Cigarette wrapper with nanoparticle spinel ferrite catalyst and methods of making same, International Patent, Publication No. WO/2005/039330, 2005.
14. Lin B, Zhang W, Liu Y, Li S, Li N. Cu-Al/Ce-Al complex oxide combustion catalysts, their preparation and use, United States Patent No. 6596249, 2003.
15. Doroftei C, Leontie L. Synthesis and characterization of some nanostructured composite oxides for low temperature catalytic combustion of dilute propane. RSC ADVANCES, 2017; 7: 27863–27871.
16. Doroftei C, Popa PD, Rezlescu N. The influence of the heat treatment on the humidity sensitivity of magnesium nanoferrite. J. Optoelectron. Adv. Mater. 2010; 12: 881–884.
17. Doroftei C. Formaldehyde sensitive Zn-doped LPFO thin films obtained by rf sputtering. SENSORS AND ACTUATORS B-CHEMICAL. 2016; 231: 793–799.
18. Doroftei C, Popa PD, Rezlescu E, Rezlescu N. Nanocrystalline SrMnO<sub>3</sub> powder as catalyst for hydrocarbon combustion. JOURNAL OF ALLOYS AND COMPOUNDS. 2014; 584:195–198.
19. Rezlescu N, Rezlescu E, Popa PD, Doroftei C, Ignat M. Nanostructured GdAlO<sub>3</sub> perovskite, a new possible catalyst for combustion of volatile organic compounds. J. Mater. Sci. 2013; 48: 4297–4304.
20. Rezlescu N, Rezlescu E, Popa PD, Doroftei C, Ignat M. Partial substitution of manganese with cerium in SrMnO<sub>3</sub> nanoperovskite catalyst. Effect of the modification on the catalytic combustion of dilute acetone. Mat. Chem. Phys. 2016; 182: 332–337.
21. Nikolica MV, Krsticb JB, Labusc NJ, Lukovica MD, Dojcinovica MP, et al. Structural, morphological and textural properties of iron manganite (FeMnO<sub>3</sub>) thick films applied for humidity sensing. Materials Science & Engineering B 2020; 257: 114-547.
22. Rayaprol S, Kaushik SD. Magnetic and magnetocaloric properties of FeMnO<sub>3</sub>. Ceramics International. 2015; 41: 9567–9571.
23. Rayaprol S, Ribeiro RAP, Singh K, Reddy VR, Kaushik SD, et al. Experimental and theoretical interpretation of magnetic

- ground state of  $\text{FeMnO}_3$ . *Journal of Alloys and Compounds*. 2019; 774: 290–298.
24. <https://www.cryst.ehu.es/magndata/index.php?index=0.508> (accessed on 19 January 2024).
  25. Rayaprol S, Kaushik SD, Babu PD, Siruguri V. Structure and magnetism of  $\text{FeMnO}_3$ . *AIP Conf. Proc.* 2013; 1512: 1132–1133.
  26. Vasiljevic ZZ, Dojcinovic MP, Krstic JB, Ribic V, Tadic NB, et al. Synthesis and antibacterial activity of iron manganite ( $\text{FeMnO}_3$ ) particles against the environmental bacterium *Bacillus subtilis*. *RSC Adv.* 2020; 10: 13879–13888.
  27. Battiston AA, Bitter JH, Heijboer WM, de Groot FMF, Koningsberger DC. Reactivity of Fe-binuclear complexes in over-exchanged Fe/ZSM5 studied by in situ XAFS spectroscopy. *Journal of Catalysis*. 2003; 215: 279–293.
  28. Han Y, Xu J, Xie W, Wang Z, Hu P. Comprehensive Study of Oxygen Vacancies on the Catalytic Performance of ZnO for CO/H<sub>2</sub> Activation Using Machine Learning–Accelerated First-Principles Simulations. *ACS Catal.* 2023; 13: 5104–5113
  29. Li M, Xu W, Wang W, Liu Y, Cui B, et al. Facile synthesis of specific  $\text{FeMnO}_3$  hollow sphere/graphene composites and their superior electrochemical energy storage performances for supercapacitor. *J Power Sources*. 2014; 248: 465–473.
  30. Lobo LS, Rubankumar A. Investigation on structural and electrical properties of  $\text{FeMnO}_3$  synthesized by sol-gel method. *Ionics*. 2019; 25: 1341–1350.
  31. Bin H, Yao Z, Zhu S, Zhu C, Pan H, et al. A high-performance anode material based on  $\text{FeMnO}_3$ /graphene composite. *Journal of Alloys and Compounds*. 2017; 695: 1223–1230.
  32. Audi AA, Sherwood P. Valence-band x-ray photoelectron spectroscopic studies of manganese and its oxides interpreted by cluster and band structure calculations. *Surf. Interface Anal.* 2002; 33: 274–282.
  33. Tang Q, Jiang L, Liu J, Wang S, Sun G. Effect of surface manganese valence of manganese oxides on the activity of the oxygen reduction reaction in alkaline media. *ACS Catal.* 2014; 4: 457–463.

34. DENG Qian, LI Xiao-mei, PENG Zhen-shan, LONG Yun-fei, XIANG Long-ming, et al. Catalytic performance and kinetics of Au/ $\gamma$ -Al<sub>2</sub>O<sub>3</sub> catalysts for low-temperature combustion of light alcohols. *Trans. Nonferrous Met. Soc. China*. 2010; 20: 437–442.
35. Avgouropoulos G, Oikonomopoulos E, Kanistras D, Ioannides T. Complete oxidation of ethanol over alkali-promoted Pt/Al<sub>2</sub>O<sub>3</sub> catalysts. *Appl. Catal. B* 2006; 65: 62–69.
36. Ivanov DV, Pinaeva LG, Sadovskaya EM, Isupova LA. Influence of the mobility of oxygen on the reactivity of La<sub>1-x</sub>Sr<sub>x</sub>MnO<sub>3</sub> perovskites in methane oxidation, *Kinetics and Catalysis*. 2011; 52: 401–408.
37. Doroftei C. Nanostructured perovskites for catalytic combustion, in *Nanostructures book*, IntechOpen, London, United Kingdom, ISBN: 978-1-78985-739-9, 2019; 5: 75–93.
38. Feng S, Yang W, Wang Z. Synthesis of porous NiFe<sub>2</sub>O<sub>4</sub> microparticles and its catalytic properties for methane combustion. *Mater Sci Eng*. 2011; 176: 1509–1512.
39. Hea L, Fan Yilin, Belletre J, Yue J, Luo L. A review on catalytic methane combustion at low temperatures: Catalysts, mechanisms, reaction conditions and reactor designs. *Renewable and Sustainable Energy Reviews*. 2020; 119: 109-589.
40. Milt VG, Ulla MA, Lombardo EA. Cobalt-containing catalysts for the high-temperature combustion of methane. *Catal. Lett*. 2000; 65: 67–73.
41. Milt VG, Spretz R, Ulla MA, Lombardo EA, Garcia Fierro JL. The nature of active sites for the oxidation of methane on La-based perovskites, *Catalysis Letters*. 1996; 42: 57–63.
42. Hammami R, Aissa SB, Batis H. Effects of thermal treatment on physico-chemical and catalytic properties of lanthanum manganite LaMnO<sub>3+y</sub>, *Applied Catalysis A: General* 353. 2009; 145–153.
43. Cicmanec P, Kotera J, Vaculík J, Bulánek R. Influence of Substrate Concentration on Kinetic Parameters of Ethanol Dehydration in MFI and CHA Zeolites and Relation of These Kinetic Parameters to Acid–Base Properties. *Catalysts*. 2022; 12: 1–15.

44. Song KS, Klvana D, Kirchnerova J. Kinetics of propane combustion over  $\text{La}_{0.66}\text{Sr}_{0.34}\text{Ni}_{0.3}\text{Co}_{0.7}\text{O}_3$  perovskite. *Appl Catal A*. 2001; 213: 113–121.
45. Cimino S, Pirone R, Lisi L. Zirconia supported  $\text{LaMnO}_3$  monoliths for the catalytic combustion of methane. *Appl Catal B*. 2002; 35: 243–254.
46. Baiker A, Marti PE, Keusch P, Fritsch E, Reller A. Influence of the A-site cation in  $\text{ACoO}_3$  ( $A = \text{La}, \text{Pr}, \text{Nd}, \text{and Gd}$ ) perovskite-type oxides on catalytic activity for methane combustion. *J. Catal.* 1994; 146: 268–276.